Master of Science Thesis in Automatic Control
Department of Electrical Engineering, Linköping University, 2016

Automatic headlight levelling using inertial measurements

Philip Nilsson

LINKÖPING
UNIVERSITY

Master of Science Thesis in Automatic Control

Automatic headlight levelling using inertial measurements

Philip Nilsson

LiTH-ISY-EX–16/4969–SE

Supervisor: **M.Sc. Martin Lindfors**
ISY, Linköpings universitet
M.Sc. Adam Claesson
Scania CV AB

Examiner: **Professor Anders Hansson**
ISY, Linköpings universitet

Division of Automatic Control
Department of Electrical Engineering
Linköping University
SE-581 83 Linköping, Sweden

Sammanfattning

För att få använda kraftiga strålkastare på lastbilar krävs att nivån på strålkastarna regleras automatiskt. Detta görs för att undvika att lastbilens strålkastare bländar andra trafikanter samtidigt som god sikt upprätthålls. För strålkastare med en ljusstyrka över 2000 lumen måste denna reglering ske automatiskt. Den huvudsakliga anledningen till att strålkastarna ändrar riktning är att lastbilens fjädring trycks ihop då lastbilen lastas. Detta resulterar i att stålkastarna pekas antingen uppåt eller nedåt beroende på hur bilen lastas.

På grund av inneboende begränsningar hos Scanias lastbilar är de vanligaste metoderna för att uppskatta hur fordonet lutar inte möjliga att implementera. Därför undersöks och presenteras en uppsättning metoder för att skatta lastbilens lutning relativt vägbanan. Tre metoder som alla innefattar användandet av sensorer som känner av acceleration väljs ut för ytterliggare utveckling. Slutligen presenteras en metod som använder sig av en kombination av en accelerationssensor och på förhand uppmätt information om väglutning för att skatta lastbilens lutning relativt vägbanan. Denna metod visas även kapabel till att producera en lutningsskattning av hög kvalitet.

Abstract

In order to use high power headlights on heavy duty vehicles, an automatic mechanism for adjusting the level of the headlights must be used. This is in order to avoid glare while still maintaining good visibility. For headlights exceeding 2000 lumen, this control must be done automatically. The main reason for a change in the headlight level is when the truck is being loaded, and the suspension is compressed causing the headlights to point slightly up or down.

Due to inherent limitations of the Scania trucks, the most commonly used approach of estimating the vehicle pitch angle is not possible to implement. Thus, a set of pitch estimation methods largely using sensors detecting acceleration are investigated and presented. Further, three methods are chosen for further study and evaluation. One method using previously recorded data about road slope as well as an on board acceleration sensor is shown to produce a high quality vehicle pitch estimate.

Contents

Notation

Notation	Meaning
θ	Pitch angle of vehicle relative to road surface
θ_g	Pitch angle of vehicle relative to an earth fixed coordinate system
α	Road slope angle
ϕ	Roll angle of vehicle relative to an earth fixed coordinate system

Abbreviations

Abbreviation	Meaning
HDV	Heavy Duty Vehicle
EKF	Extended Kalman Filter

1 Introduction

There is an ever increasing demand by customers for more powerful headlights for trucks. These headlights improve traffic safety as they will allow the driver better visibility when driving in adverse light conditions. Problems arise when there is oncoming traffic, as a powerful set of headlights are capable of distracting or blinding drivers in the oncoming traffic. To avoid glare, it is important that the headlights are pointed slightly downwards. By doing this, the headlights will illuminate the road ahead of the vehicle, which is their desired function, while also avoiding the problem of glare.

1.1 Background

The problem occurs when the truck is being loaded. Loading the truck will cause the vehicle pitch to change as the front and rear suspensions are not compressed to an equal amount. As a result of this, the direction of the headlight will change as well. Headlight level control is thus important in order to control the vertical direction in which the headlights are pointed. On a vehicle with active suspension this is automatically achieved, as the active suspension will keep the vehicle parallel to the ground. Therefore, the headlights will be controlled implicitly by the suspension. On vehicles not using an active suspension system, such as vehicles using leaf springs, there is a need for headlight level control. According to [16] the headlight level control system must be automatic, as opposed to being controlled by the driver, for headlights that exceed 2000 lumen.

On Scania trucks using leaf spring suspension the headlight level is controlled by using a level sensor measuring the distance between the rear axis and the chassis. From this, the pitch of the vehicle is estimated, and the headlight level controlled accordingly. This solution provides sufficient accuracy for controlling the headlight level to within the legal limits. Further improvement of the vehicle pitch estimation would however increase performance of the headlight level control, which in turn would improve safety and visibility while driving.

1.2 Purpose and limitations

The scope of this master thesis is limited to only using sensor data available on a truck using leaf spring suspension. Further, only the pitch angle variations caused by loading the truck are considered while other sources of pitch variations such as accelerations or road bumps are not. The purpose of this project is to investigate different methods for improving the level control that is currently used by using additional sensor- or modelling data. Further, a solution that could increase precision of the headlight level control with regard to load and load distribution is developed and evaluated.

1.3 Basis in literature and possible solutions

The main purpose of studying existing literature in this project is to collect different possibilities of controlling headlight level. The list below contains a number of different approaches to the problem. Further, information about modelling can be found in [7] for modelling in general. Moreover, information about vehicle specific modelling can be found in [11] and [12]. Information about sensor fusion can be found in [6].

1.3.1 Two accelerometer method

Using two accelerometers, one placed on one of the wheel axles of the vehicle and one on the chassis is a possibility. In this case, the two accelerometers are treated as being placed on two separate planes. The inclination of each plane is determined relative to the gravitational acceleration. The inclination of the vehicle relative to the road will be the difference between these two. This approach will experience problems with measurement errors due to acceleration other than the gravitational acceleration. These effects could be compensated for, for example by using sensor signals such as current vehicle speed in combination with an appropriate model. Idea from [3].

1.3.2 One accelerometer method

Modelling of the vehicle pitch is theoretically possible through usage of acceleration in the vertical and longitudinal axis combined with vehicle speed. A model of the vehicle inclination relative to gravity as well as a model with the inclination of the roadway is needed. A least squares approach can then be used to estimate the unknown model parameters, road inclination and vehicle pitch. The basic modelling principle is the assumption that vehicle speed measured at the wheels is always parallel to the road surface. Further, the accelerometer signals will relate to the vehicle pitch relative to the gravitational field. It is also possible to analytically solve the model equations for the vehicle attitude. This yields a solution where vehicle pitch is a function of acceleration in along three axes. Firstly, it is a function of the acceleration parallel to the vehicle chassis and secondly of the acceleration perpendicular to the vehicle chassis, towards the ground. Thirdly, the vehicle speed along the road surface is also needed for this solution. Idea from [10], [2], [5] and [14].

1.3.3 Range sensors

Range sensors of different types, for instance ultrasonic or laser-based, could be mounted in the front and rear of the vehicle in order to find the pitch angle of the vehicle relative to the ground. The main advantage of these types of sensors are that they will measure the distance from the ground and thus circumventing problems related to, for instance, modelling of suspension or tires. The main problem is however the robustness of these sensors. They would be mounted and operated in a heavy-duty environment where they would be susceptible to different types of blockages etc. A clear line of sight, which in general is required, can therefore not be guaranteed in all possible operating circumstances. Idea from [3].

1.3.4 GPS based road grade estimation

GPS could be used in order to find the inclination of the road profile. The idea would be to use the assumption that the vehicle mounted GPS will always move parallel to the road surface. The vehicle speed along the road surface will be given by the GPS as a vector in three dimensions relative to an earth-fixed coordinate system. Using this fact, an estimate of the road slope can be generated. Idea from [1] and [15].

1.3.5 Map Based road grade estimation

Any of the above proposed solutions could possibly be improved by additional knowledge about road inclination. Especially in the case of only estimating the angle between chassis and gravitational acceleration, knowledge of road inclination would immediately give the angle between road surface and chassis. Two main problems using this additional information exist. Firstly, how to control the headlight level on roads where the road slope is not known. Secondly, whether or not the road inclination database contains data with high enough resolution to be used in this application. Idea from [11].

1.3.6 Camera based methods

A forward facing camera could be used to evaluate the current headlight level. This information could then be used for controlling the headlight level up or down in a feedback loop. The main problem using this approach is the estimation of the headlight level from the camera footage. Other obstacles such as cars, trees or road signs will significantly affect how the camera sees the headlight level. Idea from [13].

1.3.7 Longitudinal vehicle model

The role of dynamic modelling in pitch estimation is for usage in the Kalman filters as described in chapter 3. A dynamic model capable of predicting one or more states in the Kalman filter will improve filter performance. The longitudinal vehicle model is meant to predict the vehicular acceleration state within the Kalman filter in order to provide a better estimate of the vehicular acceleration. Idea from [11].

2

Method and Modelling

2.1 Evaluation of methods and sensors

In this section, the different options for which sensors to be used are evaluated. Table 2.1 gives a short overview of the different vehicle pitch and road slope estimation methods. Further, table 2.2 contains a summary of the advantages and disadvantages of using different types of sensors.

Estimated angle	Methods
1. Chassis - Gravity	1.1 Accelerometer as angle sensor using gravitational acceleration 1.2 Integrate Gyroscope
2. Road - Gravity	2.1 GPS, using speed-vector along road in earth-fixed coordinate system. 2.2 Database of road slope
3. Chassis - Road	3.1 Mechanical level sensor 3.2 Optical level sensor 3.3 Acoustic level sensor 3.4 Two accelerometers, one chassis mounted, one axis-mounted 3.5 One accelerometer combined with vehicle speed, using the fact that the vehicle travels parallel to road 3.6 Any combination of (1) and (2)

Table 2.1: *Table showing the different approaches to estimate the road grade and vehicle pitch.*

Sensor type and method	Advantages and disadvantages
Accelerometer in two accelerometer method	+ Already existing sensor, robust solution. - Dependent on sensor quality.
Gyroscope Integration	+ Possible to use in tandem with other solutions for improving accuracy. - Subject to errors accumulating over time.
GPS	+ Possible to get accurate road slope readings. - Sensitive to disturbances and noise.
Database of road slope	+ Already implemented. - Not suitable as single solution, as not all roads are mapped.
Mechanical level sensor	+ Already implemented, solution accurate enough for legal requirements. - Complicated mounting and calibration, robustness issues.
Optical level sensors	+ High precision. - Not robust in the environment of a HDV, untested solution.
Acoustic level sensors	+ High precision. -Not robust, untested solution.
Single accelerometer	+ Already existing sensor, robust solution. - Heavily dependent on sensor quality.

Table 2.2: *Table showing the different initial advantages and disadvantages of using different methods for estimating pitch and road slope.*

2.1.1 Accelerometer and gyroscope

Accelerometers and gyroscopes used in integrated circuits like those used for automotive applications are part of a family of components known as MEMS circuits. MEMS stands for Micro-electro-mechanical System. A MEMS-accelerometer will measure the force that acts on a small mass inside of the device. This force is then used to determine the magnitude of acceleration that the device is subjected to.

The fundamental quantity being measured is the force acting on the mass, which is equal to the reaction force from the mass. Thus, it is not possible to distinguish between the force caused by gravity, and the force which stems from dynamic accelerations. Therefore, an accelerometer of this type will measure both the dynamic acceleration caused by changes in velocity and the gravitational pull of earth. Measuring the force exerted by the mass in three orthogonal axes makes it possible to determine the orientation of the sensor with respect to the earths gravitational field.

MEMS gyroscopes can be made using a number of different physical phenomena, among other the Coriolis force. The signal generated by the gyroscope will be the angular velocity around one or more axes. Typically, the accelerometer and gyroscope are built in to the same circuit and gives acceleration and angular velocity around the same axes.

Accelerometer and gyroscope as angle sensor

The basic idea of using one or more accelerometers for sensing the angle of the accelerometer itself has the distinct advantage of not suffering from drift. The gyroscope however, gives the angular speed about one or more axes. Integrating angular speed will yield an absolute angle. The integration will however also include any noise and bias present in the angular speed signal. Thus, the angle estimate will be subject to drift.

Using an accelerometer to sense the effects of the gravitational acceleration will not be subject to drift since what is measured is the contribution from gravity in one or more axes of the sensor. The angle estimate may contain noise, but will over time converge to the true mean of the measured quantity, not including bias. In practice, automotive grade accelerometers will have a significant bias that may drift over time as a function of, for instance, temperature and age.

Combining the readings from a gyroscope and and accelerometer, for instance by using a Kalman filter, will result in an accurate angle estimate. The disadvantage of doing this in an automotive context is the additional cost that a gyroscope will add. For this reason, an approach using only an accelerometer may be more desirable than a more costly and accurate solution using two different sensors.

Accelerometer combined with vehicle speed

Rather than using an accelerometer as an angle sensor, it can be used to directly estimate the pitch angle between the road and vehicle as described in 1.3.

The advantages of this solution are that it would be both reliable and inexpensive. The robustness would stem from the fact that the sensor is well protected and has no moving parts. It is therefore not affected by the harsh environment surrounding a heavy duty vehicle. Further, both the acceleration sensor and vehicle speed sensor are already parts of the current hardware, thus not adding any additional cost to the vehicle.

A clear disadvantage is the theoretical complexity of the solution. While it theoretically is fully viable, there is a clear risk of the solution being very sensitive to noisy and biased measurement signals.

2.1.2 Level sensors

Any selection of level sensors will have to operate in the environment between the vehicle chassis and roadway. The consequence of this is a need for very reliable sensors that are not easily affected by snow, mud or water. Within the choice of level sensors, the only option that fulfils this criterion is the mechanical level sensor.

The mechanical level sensors are however affected by other difficulties. Mainly, it has not been possible to find a way of mounting a level sensor on the front axis of a vehicle. It is thus necessary to use only a level sensor on the rear axis, and from this model the compression of the front suspension in order to achieve a pitch estimate. This modelling has been shown to not be trivial as there are a number of variables that are unknown.

2.1.3 GPS-based solutions

There are two main applications of GPS data for estimating the vehicle pitch angle. First, it is theoretically possible to extract the road slope by using the inclination of the speed vector derived through GPS measurements. Secondly, a possible solution would be to use a database containing the road slope for different roads. This kind of database could then be accessed in much the same way that a traditional GPS tracks position on a map, but rather than position, use it for tracking the current road slope.

2.1.4 Longitudinal vehicle model

The model is made up of 4 different parts as shown in equations (2.2) to (2.6). The net longitudinal force driving the vehicle is according to Newtonian physics described by

$$F_{net} = m\dot{v}. \tag{2.1}$$

This means that the Kalman filter will use the variable $\dot{v}$ which represents the vehicular acceleration in the time update step.

The vehicular acceleration is derived through summing the different resistive and propelling forces affecting the vehicle in motion:

$$m\dot{v} = F_{propulsion} - F_{airdrag} - F_{roll} - F_{gravity} - F_{brake}. \tag{2.2}$$

In order to accurately model the propulsion force, $F_{propulsion}$, the entire driveline needs to be modelled. As the main focus of interest in this thesis is the static pitch angle resulting from the loading of the vehicle, components such as the torsion of shafts and axles are neglected as they represent a high frequency behaviour, as described in [11].

The modelling of engine, clutch and transmission is already done internally at Scania. As the end goal of this thesis is to estimate the pitch angle of a HDV, this thorough modelling is judged to be out of scope for this paper. Therefore, the existing in-house estimate of the torque at the output shaft of the gearbox, $Tq_{transmission}$, from Scania is used directly. This combined with the radius of the driving wheels and the rear axle gear ratio, $RAGR$, will give the force propelling the HDV forward according to

$$F_{propulsion} = \frac{T_{transmission}}{r_{wheel}} \cdot RAGR. \tag{2.3}$$

The resistive contributions of the longitudinal vehicle model can be mathe-

RAGR	Rear Axle Gear Ratio	[-]
r_{wheel}	Radius of driving wheels	[m]
$T_{transmission}$	Torque at output shaft of transmission	[Nm]
C_d	Air resistance coefficient	[-]
A_{front}	Frontal area of vehicle	[m^2]
ρ_a	Air density	[kg/m^3]
v	Vehicle speed	[m/s]
m	Vehicle mass	[kg]
c_r	Rolling resistance coefficient	[-]
α	Road slope	[rad]

Table 2.3: *Explanation of variables in equations* (2.2) *to* (2.6).

matically described by

$$F_{airdrag} = \frac{1}{2} C_d A_{front} \rho_a v^2, \tag{2.4}$$

$$F_{roll} = mgc_r \cos \alpha, \tag{2.5}$$

$$F_{gravity} = mg \sin \alpha. \tag{2.6}$$

This section aims to evaluate the plausibility of the previously described vehicle model with respect to their potential usability in vehicle pitch estimation. In order to evaluate the longitudinal vehicle model two signals from the vehicle control units were examined. Firstly, there is a signal which contains the torque applied to the output shaft of the transmission. Secondly, there is a signal with the estimated driving resistances as described in section 1.3.7. The equation

$$F_{prop} = \frac{Tq_{transmission}}{r_{wheel}} \cdot RAGR \tag{2.7}$$

and table 2.3 shows how the total propulsion force is generated from the transmission output torque.

Further,

$$m \cdot a = F_{prop} - F_{res} \tag{2.8}$$

shows the composition of the complete longitudinal vehicle model. In order to use this model for estimating the vehicular acceleration the mass needs to be estimated. On HDV:s the weight is conventionally estimated either by the air suspension system or through modelling such as the longitudinal vehicle model described in this paper or other similar methods [4].

This means that modelling the longitudinal acceleration of an HDV requires a way of estimating the vehicle mass which does not already rely on using a longitudinal acceleration model. Thus, the longitudinal vehicle acceleration model might be of use for designing an automatic headlight levelling system on a vehicle equipped with an air suspension system. This would however be outside of the scope of this thesis.

2.2 Methods chosen for further development

The following methods are the ones chosen for further development. The choices are motivated and explained using the previously mentioned advantages and disadvantages.

2.2.1 One accelerometer method

The method of estimating vehicle pitch using a single accelerometer mounted on the frame of the vehicle was chosen for further development. Assuming the method to be practically viable the advantages of only using sensors already mounted on vehicles are significant. This fact in combination with previous work suggesting it might be a viable solution motivates the further development of this method.

2.2.2 Two accelerometer method

The two accelerometer method described in 1.3 was also chosen for further development. This was in large due to the theoretical simplicity of the solution. The method based on one accelerometer is as previously discussed a rather complex method theoretically. Using an additional accelerometer adds hardware complexity, but is not as complex with respect to measurement equations or dynamics.

2.2.3 Map data

Using map data for estimating pitch has the distinct advantage of only using standard sensors already available on Scania trucks. The road slope estimate is also a reliable signal with high precision when driving on previously mapped roads. This in combination with the potential possibility of augmenting the previously mentioned methods with the information contained in the road slope data means that this method is to be investigated further.

3
Estimation

This chapter aims to give the theory used for the estimation of vehicle pitch for the different methods that have been investigated. The vehicle coordinate system is shown in figure 3.1, with the x-axis pointing in the direction of travel. The y-axis is directed to the left of the vehicle and the z-axis is directed straight up.

Further, the road slope angle is denoted α and the vehicle pitch angle relative to the road is denoted θ. In situations where the angle of interest is the pitch angle relative to an earth fixed coordinate system, the pitch angle will include an extra subscript, θ_g.

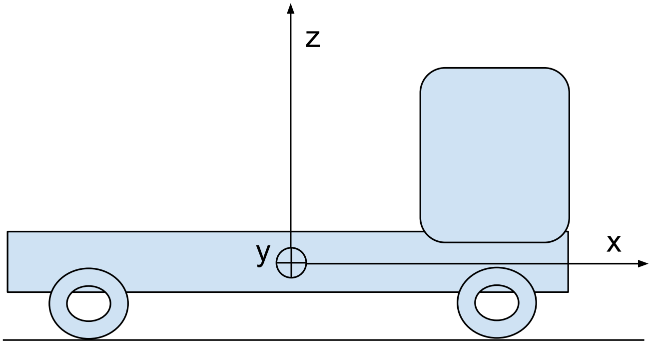

Figure 3.1: *Figure describing the vehicle fixed coordinate system.*

3.1 Kalman Filtering

The Kalman filter is an algorithm that uses both measured and modelled information about a system in order to produce a state estimate. [6] gives a thorough explanation of Kalman filters and their use. Normally, a Kalman filter is a linear state estimator described by its measurement and time update equations. Since the models described in this thesis are to a large extent non-linear, the extended Kalman filter, abbreviated EKF, will be used.

The extended Kalman filter has the advantage of being able to use non linear time update and measurement equations, according to

$$x_k = f(x_{k-1}, u_k) + w_k \tag{3.1}$$

$$z_k = h(x_k) + e_k. \tag{3.2}$$

Here, x are the states estimated by the filter, z the measurements and u any control signal or input to the filter. In each time step, these equations are linearised as described in [6]. w_k and e_k are the process and observation noise respectively both assumed to be zero mean Gaussian noise distributions. At each time step, the future states are predicted by the use of the function f. The function h is then used to estimate the predicted measurements based on the predicted states.

As the extended Kalman filter linearises the non-linear measurement equations in each time step, the optimality of the linear Kalman filter is lost. For a non linear system that is approximately linear on the scale of the time steps used, the first order EKF as described in this thesis will work [6]. The first order extended Kalman filter will ,however, start producing results that are increasingly poor as the non-linearity of the states estimated increase. In this case, alternative methods such as a higher order or unscented Kalman filter could be better options [6].

3.2 One accelerometer method

Figure 3.2 shows the relevant quantities used in the one accelerometer pitch estimation method. The relevant quantities are also listed in table 3.1.

θ_g	Pitch angle relative to gravity
θ	Pitch angle relative to road surface
α	Road slope angle
$\dot{v}$	Vehicular acceleration

Table 3.1: *Essential variables for the one accelerometer pitch estimation method.*

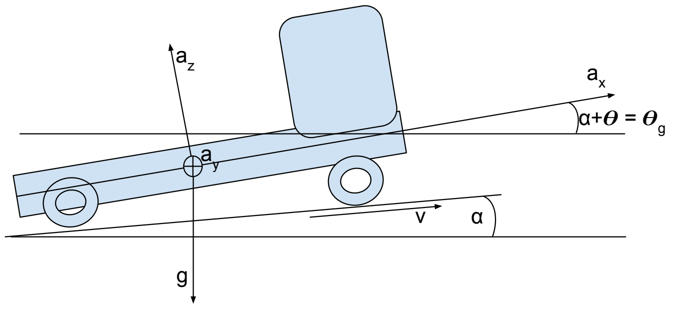

Figure 3.2: *Figure describing the quantities involved in the vehicle pitch estimation.*

The states present in the EKF for the one accelerometer method are the vehicular acceleration, road slope and vehicle pitch angle as given by

$$x_1 = \dot{v}, \tag{3.3}$$

$$x_2 = \alpha, \tag{3.4}$$

$$x_3 = \theta. \tag{3.5}$$

The measurement equations used for pitch estimation for the one accelerometer method can be written as

$$z_1 = a_x = \dot{v}\cos(\theta) + g\sin(\alpha + \theta) + e_{a_x}, \tag{3.6}$$

$$z_2 = a_z = -\dot{v}\sin(\theta) + g\cos(\alpha + \theta) + e_{a_z}, \tag{3.7}$$

$$z_3 = \dot{v} + e_{\dot{v}} \tag{3.8}$$

where e_{a_x}, e_{a_z} and $e_{\dot{v}}$ represent the noise present in the measured signals.

The equations are comprised of two contributions, one from the vehicular acceleration and one from the gravitational acceleration. As can be seen in the measurement equations, this approach is dependent on the presence of the vehicular acceleration $\dot{v}$. This can be found partly when the vehicle is accelerating or decelerating as a response to changing driving circumstances such as speed limitations or traffic. Further, $\dot{v}$ will vary around the desired speed during stationary driving. These changes in speed are what makes it theoretically possible to estimate the vehicle pitch.

All states are in the time update modelled as random walks

$$\dot{v}_k = \dot{v}_{k-1} + w_{\dot{v},k}, \tag{3.9}$$

$$\alpha_k = \alpha_{k-1} + w_{\alpha,k}, \tag{3.10}$$

$$\theta_k = \theta_{k-1} + w_{\theta,k} \tag{3.11}$$

where the addition of noise w_k allows the estimates to change over time. This is done because of the assumption that both the pitch and road slope angles will change very slowly, if at all. The effect of fast variations in pitch caused by things such as road irregularities and hard braking can thus mitigated through this approach with an appropriate choice of covariance matrices in the Kalman filter.

3.2.1 Derivation of measurement equations

Measurement equation for acceleration in the x-axis

The accelerometer will in the vehicular x-axis sense an acceleration according to

$$z_1 = a_x = a_{x,vehicle} + a_{x,gravity}. \tag{3.12}$$

In this equation, two contributions together form the acceleration in the vehicular x-axis. Firstly, there is the acceleration component stemming from the vehicular acceleration. Assuming a pitch angle of zero degrees, all of the vehicular acceleration would be sensed by the accelerometer in the x-axis. Introducing a nonzero pitch angle, $\theta \neq 0$, will mean that the vehicular acceleration is increasingly sensed by the accelerometer in the z-axis. Therefore, the x-axis contribution of the vehicular acceleration is estimated as

$$a_{x,vehicle} = \dot{v}\cos\theta. \tag{3.13}$$

Secondly, there is the contribution from the gravitational pull on the accelerometer. If both the road slope and pitch angles are zero, the full gravitational pull will be detected in the z-axis of the accelerometer, with the component in the x-axis being zero. As the pitch angle relative to gravity becomes non-zero, $\theta_g \neq 0$, the x-axis of the accelerometer will increasingly be affected by gravity. Thus, the x-axis contribution from gravity is estimated as

$$a_{x,gravity} = g\sin\theta_g. \tag{3.14}$$

Combining equations (3.12) to (3.14) gives the measurement equation in the x-axis as in equation (3.6).

Measurement equation for acceleration in the z-axis

Acceleration as perceived by the accelerometer in the z-axis can be described as

$$z_2 = a_z = a_{z,vehicle} + a_{z,gravity}. \tag{3.15}$$

Much like in the x-axis, the acceleration sensed by the accelerometer in the z-axis consists of two parts, one stemming from gravitational and one stemming from vehicular acceleration.

The vehicular acceleration, $\dot{v}$, as sensed by the accelerometer in the z-axis will be scaled by $-\sin\theta$. This is because an increase in the pitch angle will result in a negative acceleration with a coordinate system such as in figure 3.1 and 3.2. This gives the component $a_{z,vehicle}$ according to

$$a_{z,vehicle} = -\dot{v}\sin\theta. \tag{3.16}$$

Further, the gravitational component of the acceleration in the z-axis will be scaled by a factor of $\cos\theta_g$, giving $a_{z,gravity}$ according to

$$a_{z,gravity} = g\cos\theta_g. \tag{3.17}$$

Measurement equation for the vehicular acceleration

The vehicular acceleration is a directly measured quantity in the Kalman filter, therefore the last of the measurement equations is written as

$$z_3 = \dot{v}. \tag{3.18}$$

3.3 Two accelerometer method

This method relies upon two sets of measurement equations, one set for each accelerometer. The accelerometer orientation can either be estimated in two or three dimensions. In the two dimensional case, only the x and z-axes of the accelerometer are used whereas the three-dimensional case will use data from all three axes.

For the two dimensional case, only one state which represents the pitch angle relative to gravity,

$$x = \theta_g \tag{3.19}$$

is used. In the three dimensional case however, two states need be used according to

$$x_1 = \theta_g, \tag{3.20}$$

$$x_2 = \phi_g \tag{3.21}$$

where ϕ_g represents the roll angle around the x-axis relative to gravity.

The advantage of using the two dimensional approach is that the measurement equations become simpler than in the three dimensional case. Further, the three dimensional approach will experience noise from the lateral accelerometer axis. This may or may not decrease estimation performance, depending on the signal to noise ratio for the specific driving scenario.

In the two dimensional case, the lateral component of the acceleration is neglected. This gives the measurement equations described by

$$z_1 = a_x = -\sin\theta_g + e_{a_x} \tag{3.22}$$

$$z_2 = a_z = \cos\theta_g + e_{a_z}. \tag{3.23}$$

These measurement equations allows for estimation of the orientation of each of the individual accelerometers through the use of the extended Kalman filter.

In the three dimensional case however, the lateral component of the acceleration is used. This means estimating not only the pitch, but also the roll angle of the vehicle, as can be seen in the measurement equations described by

$$z_1 = a_x = -\sin\theta_g + e_{a_x}, \tag{3.24}$$

$$z_2 = a_y = \cos\theta_g \sin\phi_g + e_{a_y}, \tag{3.25}$$

$$z_3 = a_z = \cos\theta_g \cos\phi_g + e_{a_z}. \tag{3.26}$$

The dynamics are modelled to be constant with time update equations according to

$$\theta_{g,k} = \theta_{g,k-1} + w_{\theta_g,k}, \tag{3.27}$$

$$\phi_{g,k} = \phi_{g,k-1} + w_{\phi_g,k} \tag{3.28}$$

for the three dimensional method, or

$$\theta_{g,k} = \theta_{g,k-1} + w_{\theta_g,k} \tag{3.29}$$

for the two dimensional method. In the same way as for the one accelerometer method, the noise term w_k will allow the pitch estimate to vary and can thus be used as a tuning parameter in the EKF.

3.3.1 Derivation of measurement equations

The measurement equations for the two accelerometer method are the result of a series of rotations about the x and y-axis of the vehicle. The amount of rotation around the different axes will represent the pitch and roll angles of the vehicle.

Two dimensions

In order to obtain an orientation estimate using the gravitational pull on a three axis-accelerometer, the gravitational acceleration indicated by the accelerometer is treated as a three-dimensional vector. Assuming no dynamic acceleration is applied to the accelerometer, the vector will be pointing straight towards the earth according to

$$g = \begin{pmatrix} 0 \\ 0 \\ g \end{pmatrix}. \tag{3.30}$$

The gravitational vector is measured upwards along the positive z-axis due to the physical construction of the accelerometer, as explained in chapter 2.

Would the accelerometer be subject to accelerating motion, the accelerometer readings would contain this acceleration as well thus making the accelerometer assume a different gravitational vector as

$$g_{motion} = \begin{pmatrix} 0 + a_{x,dyn} \\ 0 + a_{y,dyn} \\ g + a_{z,dyn} \end{pmatrix}. \tag{3.31}$$

Normalising the gravitational vector in equation (3.30) to unit length will yield

$$g_{normalised} = \begin{pmatrix} 0 \\ 0 \\ 1 \end{pmatrix}. \tag{3.32}$$

This is done because of the inherent bias that is present on automotive grade accelerometers. The actual size of the measured acceleration is not what is sought, but rather the direction of acceleration. There will still be some bias affecting the normalised accelerometer readings. Such bias stems from the fact that all accelerometer axes are not perfectly orthogonal to each other, but will pick up on some acceleration in axes other than their own.

The accelerometer detects acceleration in its own three axes, rather than in an earth fixed coordinate system. Thus, the measurement equations (3.6) to (3.8) are a result of a series of rotations, which aims to rotate the perceived acceleration vector in line with the earth fixed one, (3.30). Since the pitch angle is represented by a rotation around the y-axis of the vehicle, the rotation of the gravitational vector can be written as per

$$R_y = \begin{pmatrix} cos(\theta_g) & 0 & -sin(\theta_g) \\ 0 & 1 & 0 \\ sin(\theta_g) & 0 & cos(\theta_g) \end{pmatrix}. \tag{3.33}$$

Here, the angle θ_g represents the pitch angle of the accelerometer relative a earth fixed coordinate system. Performing the multiplication of the rotational matrix R_y with the gravitational vector gives the measurement equations as

$$R_y \cdot g = \begin{pmatrix} -sin(\theta_g) \\ 0 \\ cos(\theta_g) \end{pmatrix}. \tag{3.34}$$

Three dimensions

In the three dimensional case, the pitch and roll angles will have an interdependence in the y and z-axes. Thus, information from the y-axis can in theory contribute to an increase in estimation performance. In order to expand the two dimensional case into three dimensions, the rotational matrix R_x is multiplied onto the measurement equations of the two dimensional case. R_x is the rotational matrix about the x-axis of the vehicle as described by

$$R_x = \begin{pmatrix} 1 & 0 & 0 \\ 0 & cos(\phi_g) & sin(\phi_g) \\ 0 & -sin(\phi_g) & cos(\phi_g) \end{pmatrix} \tag{3.35}$$

corresponding to a rotation matrix for the roll angle ϕ.

The rotations described by

$$R_x \cdot R_y \cdot g = \begin{pmatrix} -sin(\theta_g) \\ cos(\theta_g)sin(\phi_g) \\ cos(\theta_g)cos(\phi_g) \end{pmatrix} \tag{3.36}$$

shows the measurement equations for the three dimensional case of the two accelerometer method for estimating the accelerometer pitch and roll angles.

The gain of using the three dimensional measurement equations is however very limited since θ_g is small, thus rendering the cosine approximately equal to one:

$$\cos\theta_g \approx 1. \tag{3.37}$$

3.3.2 Linearisation of measurement equations

An implementation on an actual truck will require the Kalman filter to be operating in real time on a control unit in the truck. Resource efficiency would in this case be essential and one way of achieving an increase in efficiency is to linearise the measurement equations of the Kalman filters. This means a normal, linear, Kalman filter can be used rather than the EKF described in section 3.1.

Equations (3.38) to (3.39) shows the commonly used small angle approximation of the cosine and sine functions when measuring the angles in radians. As a vehicle pitch angle of only a few degrees is considered as significant, this small angle approximation is used:

$$\cos x = 1, \tag{3.38}$$

$$\sin x = x. \tag{3.39}$$

The linearised measurement equations for the two accelerometer method in 3 dimensions are described by

$$a_x = -\theta_g, \tag{3.40}$$

$$a_y = 1 \cdot \phi_g, \tag{3.41}$$

$$a_z = 1 \cdot 1. \tag{3.42}$$

By looking at these equations, it becomes clear that the measurement equations for the two accelerometer method in the linear case could be reduced to a single equation as per

$$z = a_x = -\theta_g. \tag{3.43}$$

3.3.3 Aligning coordinate systems of accelerometers

When mounting an accelerometer to the rear axle of an HDV, the options for the physical mount are limited. This means that it is not possible to reliably mount the accelerometer in a way where it is parallel to the ground. Because of this, a method for aligning the coordinate systems of the frame and axle mounted accelerometer is needed. This is called Wahba's problem and solutions were presented in [8] and [9].

The idea in this case is to rotate the measurements from the axle mounted accelerometer to express them in the coordinate system of the frame mounted accelerometer. For this, the vehicle is positioned in a zero pitch attitude on a horizontal surface. The acceleration vector will then be pointing straight down, in the direction of the gravitational acceleration. In the two coordinate systems of the accelerometers, the gravitational acceleration vector will be expressed differently. Thus, what is needed is the rotational matrix A that rotates the axle mounted accelerometer readings to align them with the readings of the frame mounted accelerometer. A multiplication of each measured vector $\bar{a}_{measured,i}$ from the axle mounted accelerometer such as

$$A \cdot \bar{a}_{measured,i} = \bar{a}_{rotated,i} \tag{3.44}$$

will yield rotated measurements $\bar{a}_{rotated,i}$. The rotated measurements are then expressed in the coordinate system of the frame mounted accelerometer.

3.4 Map data

As described in chapter 1, a database containing the road slope angles can be used in order to augment the one and two accelerometer methods. Primarily, it can be used as one more measured value in the one accelerometer method. Thus, the states for the map based pitch estimation method are again chosen according to equations (3.3) to (3.5). Adding the extra information about road slope to the measurement equations of the one accelerometer method yields a new set of measurement equations given by

$$z_1 = a_x = \dot{v}\cos(\theta) + g\sin(\alpha + \theta) + e_{a_x}, \tag{3.45}$$

$$z_2 = a_z = -\dot{v}\sin(\theta) + g\cos(\alpha + \theta) + e_{a_z}, \tag{3.46}$$

$$z_3 = \dot{v} + e_{\dot{v}}, \tag{3.47}$$

$$z_4 = \alpha + e_{\alpha}. \tag{3.48}$$

Further, the dynamics of the map based pitch estimation method are again modelled as constants, as for the one accelerometer method in equation (3.9) to (3.9). The added information in the measurement equations does however require a different approach to tuning the covariance matrices in the EKF. Because of the high quality expected of the road slope data in the fourth measurement, the measurement noise can be assumed to be very low for this measurement equation. This will result in the Kalman filter not filtering the road slope angle as much as the other measurement signals. Thus, an increase in pitch estimation performance is expected.

The road slope acquired from the map database could also be used in order to eliminate one of the accelerometers in the two accelerometer method. In this case, only one set of measurement equations for pitch estimation would be needed in order to estimate the pitch angle of the vehicle relative to gravity. The road slope data can then be subtracted from the vehicle pitch angle relative to gravity, which will yield an estimate of the pitch angle between the vehicle and the road surface.

4

Simulation and results

In order to validate the theoretical reasoning from chapter 3, a short simulation study has been carried out. The main goal is to validate the measurement models and the filters designed from theoretical reasoning. Further, a deepened insight into the plausibility of the different methods is to be gained.

In the cases where there is an option of estimating the vehicle pitch angle in two or three dimensions, only the two dimensional cases are simulated. Simulating the lateral acceleration of the vehicle would require modelling of yet another type and is thus deemed as being out of the scope of this thesis.

4.1 Accelerometer noise analysis

In order to assess the plausibility of different methods of vehicle pitch estimation, noise will be introduced to the simulations. Therefore, an analysis of the noise present in the accelerometer readings has been carried out. Figure 4.1 shows a normal probability plot of the acceleration output from a vehicle mounted accelerometer. The data is collected from a truck at standstill with the engine running. This was done in order to get a realistic amount of noise consisting both of vehicle vibrations and the inherent noise of the accelerometer.

In a normal probability plot such as 4.1, the data points will be plotted along a straight line if the data is normally distributed. As can be seen, the data is mostly normally distributed. Thus, an addition of noise that is normally distributed will approximate the actual noise that an accelerometer is subjected to.

Further, the standard deviation and variance of the accelerometer signal in the different axes can be seen in table 4.1.

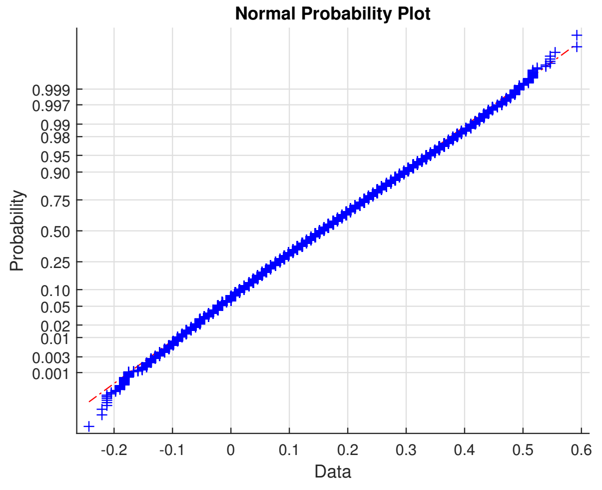

Figure 4.1: *Normal probability plot of accelerometer data collected from a truck at standstill with the engine running at idle.*

Axis	σ	σ^2
X	0.1088	0.0118
Y	0.1066	0.0114
Z	0.1046	0.0109

Table 4.1: *Standard deviation and variance of accelerometer signals when mounted on a truck at standstill with engine running.*

4.2 One accelerometer method

The first step in simulating the one accelerometer method was to do so without the presence of noise in order to illustrate that the vehicle pitch angle is in fact identifiable. Noise was then added, first in the accelerometer readings, and lastly in the vehicular acceleration signal. The acceleration in the x and z-axes was simulated through the measurement equations described in chapter 3 by using constant road slope and vehicle pitch angles as input signals. Table 4.2 shows the constant reference values used when generating the simulated accelerometer data.

Pitch [°]	Road Slope [°]
1	4

Table 4.2: *Simulation input values for vehicle pitch and road slope.*

4.2.1 Simulation without noise

A signal representing the vehicle acceleration was generated as a sine function. Figure 4.2 shows the vehicular acceleration as well as the road slope and vehicle pitch angles for the noiseless case. As can be seen, both the road slope and pitch angles converge towards the correct values given an excitation of the vehicular acceleration. In the noiseless case, the speed of which the estimates converge is heavily dependent on how the EKF is tuned with respect to process and measurement noise.

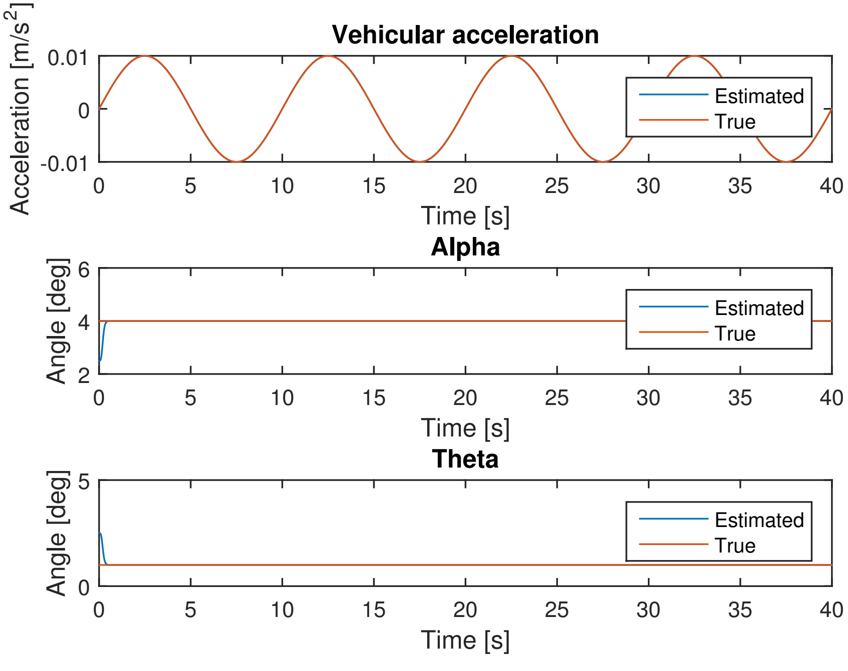

Figure 4.2: Simulation results for the one accelerometer method without added noise.

Filter parameters

In order to produce the simulation results as shown in figure 4.2 the EKF was tuned to be relatively fast. This was done as the simulation did not contain any noise which might need to be filtered. The observation and process covariance matrices were

$$R = Q = \begin{pmatrix} 1 & 0 & 0 \\ 0 & 1 & 0 \\ 0 & 0 & 1 \end{pmatrix}. \tag{4.1}$$

The initial states were

$$x_0 = \begin{pmatrix} \dot{v}_0 \\ \alpha_0 \\ \theta_0 \end{pmatrix} = \begin{pmatrix} 0 \\ 0 \\ 0 \end{pmatrix} \tag{4.2}$$

as there in a realistic driving situation is no way of knowing the initial states before start of driving using this pitch estimation method. Further, the initial covariance matrix was chosen as

$$P_0 = 0.5 \cdot \begin{pmatrix} 1 & 0 & 0 \\ 0 & 1 & 0 \\ 0 & 0 & 1 \end{pmatrix} \tag{4.3}$$

since this will correspond to a standard deviation of approximately 10 degrees.

4.2.2 Simulation with accelerometer noise

Adding noise of a realistic size in the x and z-axes gives the results as described by figure 4.3. The simulation results are further quantified in table 4.3. As is evident by figure 4.3 and table 4.3, the one accelerometer method has an inherent sensitivity to noise. Further, the simulation carried out did not contain noise in the vehicular acceleration signal. Adding noise in the measurements of the vehicular acceleration would likely make the accuracy of the vehicle pitch estimate deteriorate even more.

	Mean estimate [°]	Ground truth [°]
Road slope	3.29	4
Pitch	1.71	1

Table 4.3: *Mean values of pitch and road slope estimates from simulation of the one accelerometer method using noisy accelerometer measurements. Mean values taken from the 10 last seconds of simulation.*

Filter parameters

For the simulation of the one accelerometer method using measurement noise in the accelerometer axes, the EKF was tuned to rely heavily on the vehicular acceleration signal. This was done in order to get a pitch estimate that is as accurate as possible, as the vehicular acceleration signal is generated without noise. The measurement covariance matrix was

$$R = 10^4 \cdot \begin{pmatrix} 1 & 0 & 0 \\ 0 & 1 & 0 \\ 0 & 0 & 10^{-4} \end{pmatrix} \tag{4.4}$$

and the process noise covariance matrix was

$$Q = \begin{pmatrix} 1 & 0 & 0 \\ 0 & 10^{-3} & 0 \\ 0 & 0 & 10^{-3} \end{pmatrix}. \tag{4.5}$$

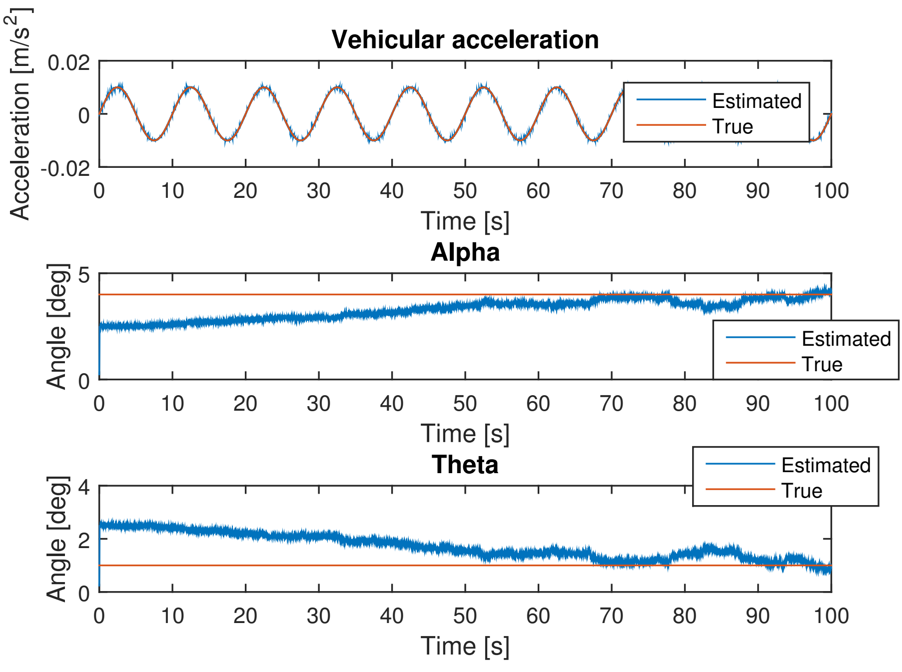

Figure 4.3: *Simulation results after adding noise in both the x and z-axes.*

Further, the initial states x_0 and covariance matrix P_0 were again chosen as in equations (4.2) and (4.3).

4.2.3 Simulation with noise in accelerometer and vehicular acceleration

In order to investigate the effect of a noisy acceleration signal, a simulation with parameters according to table 4.4 was carried out. The noise applied to the accelerometer readings remained the same size as in previous simulations, since it was deemed to be of a realistic size. Further, the noise added to the vehicular acceleration signal was also of the same character and size. This was done because of a lack of information regarding the noise in the vehicular acceleration. Further, the vehicular acceleration can be expected to display different noise characteristics depending on the driving scenario that is currently being investigated.

The results of the simulation can be seen in figure 4.4 and table 4.5. The figure clearly shows the effect of the noise on the vehicle pitch estimate.

Figure 4.5 shows the pitch estimate together with a confidence interval generated from the covariance matrix P of the extended Kalman filter. As can be seen, the confidence interval gets wider rather than more narrow as more measurements come in. This further indicates that the one accelerometer method is

State	σ	σ^2
Acceleration x-axis	0.1	0.01
Acceleration z-axis	0.1	0.01
Vehicular acceleration	0.1	0.01

Table 4.4: *Noise quantities for simulation of the one accelerometer method with noise in both accelerometer axes and vehicular acceleration.*

	Mean estimate [°]	Ground truth [°]
Road Slope	3.04	4
Pitch	1.96	1

Table 4.5: *Mean of pitch and road slope estimates from a simulation of the one accelerometer method with noise in both accelerometer axes and vehicular acceleration.*

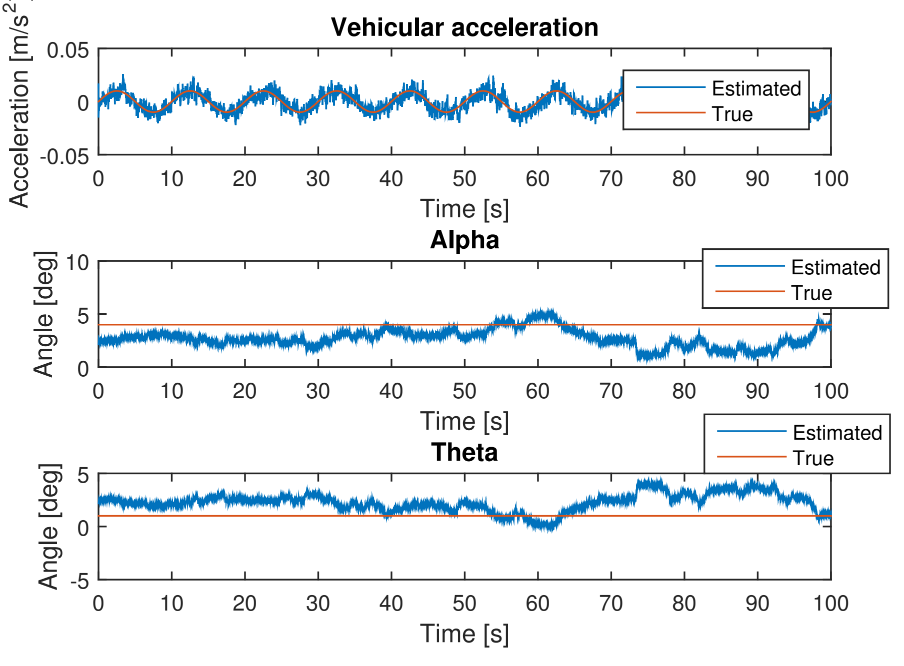

Figure 4.4: *Results from simulation of the one accelerometer method with noise in both accelerometer and vehicular acceleration measurements.*

extremely sensitive to noise as the estimate becomes increasingly unreliable.

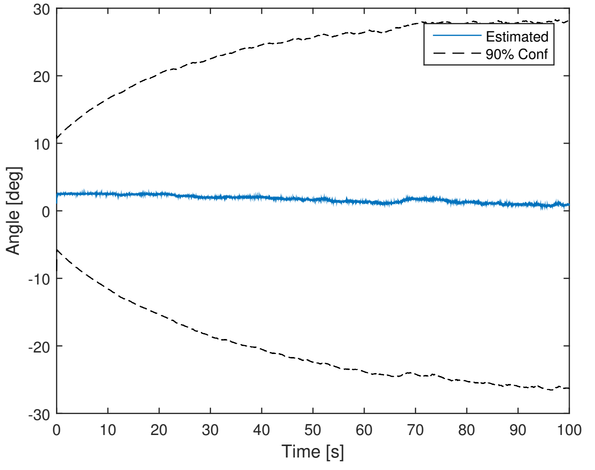

Figure 4.5: *Pitch angle estimate with a 90 % confidence interval from the simulation of the one accelerometer method with noise in all measurements.*

Filter parameters

When simulating the one accelerometer method with noise in all measurements the observation covariance matrix was

$$R = 10^3 \cdot \begin{pmatrix} 1 & 0 & 0 \\ 0 & 1 & 0 \\ 0 & 0 & 1 \end{pmatrix}. \tag{4.6}$$

The process covariance matrix was

$$Q = 10^{-3} \cdot \begin{pmatrix} 1 & 0 & 0 \\ 0 & 1 & 0 \\ 0 & 0 & 1 \end{pmatrix}. \tag{4.7}$$

The initial values for the states x_0 and covariance matrix P_0 were again chosen according to equations (4.2) and (4.3). These design choices were made as all signals are equally contaminated by noise.

4.3 Two accelerometer method

In order to evaluate the two accelerometer method, one set of the measurement equations has been simulated. This was done as a way of showing the possible accuracy of the pitch estimate from the accelerometer readings. An actual implementation of the two accelerometer method would include two sets of measurement equations, as well as a comparison between the two estimates.

4.3.1 Simulation without measurement noise

The two accelerometer measurement equations were used in order to simulate the orientation of an accelerometer. Figure 4.6 together with table 4.6 shows the simulation results without measurement noise present. As can be seen in the figure, the pitch estimate converge towards the actual pitch angle.

Mean pitch estimate [°]	Ground truth [°]
1	1

Table 4.6: *Simulation results for the two accelerometer method without measurement noise added.*

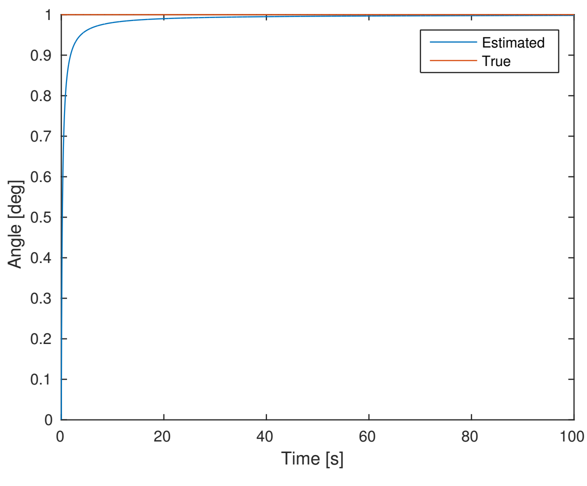

Figure 4.6: *Simulation results for the two accelerometer method without measurement noise added.*

Filter parameters

For simulation of the two accelerometer method, the initial states for the filter were chosen as $x_0 = \theta_{g,0} = 0$ and $P_0 = 0.5$. The observation noise covariance was chosen as

$$R = 10^3 \cdot \begin{pmatrix} 1 & 0 \\ 0 & 1 \end{pmatrix} \tag{4.8}$$

and the process noise covariance as $Q = 10^{-10}$. This gives, as can be seen in figure 4.6, a relatively slow filter which should be able to filter out fast variations in pitch.

4.3.2 Simulation with noise

When simulating the measurement equations from the two accelerometer method with noise added to the measurements, the same type and size of noise was used as when simulating the one accelerometer method. Table 4.7 shows the standard deviation and variance of the noise which is added both in the x and z-axes of the simulated accelerometer readings.

	σ	σ^2
x-axis	0.1	0.01
z-axis	0.1	0.01

Table 4.7: *Noise added to the measurement readings when simulating the measurement equations of the two accelerometer method*

Figure 4.7 and table 4.8 shows the results of the simulation when noise was applied to the accelerometer measurements. As can be seen from both the figure and the mean of the pitch estimate presented in the table, the pitch estimate will over time converge to the true pitch of the accelerometer. The time it takes for the pitch estimate to converge, as well as the variance of the pitch estimate can be affected through tuning of the EKF. Tuning the filter to a shorter rise time will result in a pitch estimate with larger variations around the actual pitch angle. In the same way, tuning the filter for smaller variations around the actual pitch angle will result in an increase in the rise time of the filter.

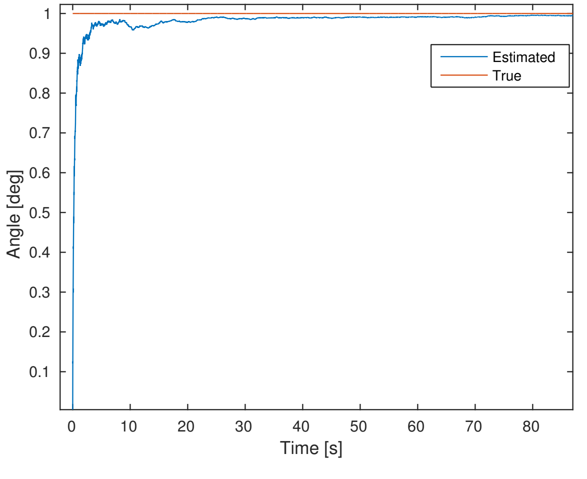

Figure 4.7: *Results from simulating measurement equations from the two accelerometer method with noise in accelerometer readings.*

Figure 4.8 shows a confidence interval around the pitch estimate. As can be seen, the confidence interval starts out relatively wide and gets increasingly narrow as more measurements are gathered.

Mean pitch estimate [°]	Ground truth [°]
1.01	1

Table 4.8: *Mean of pitch estimate from simulated results of the two accelerometer method with noise applied in the accelerometer measurements. Mean calculated from the last 10 seconds of measurement.*

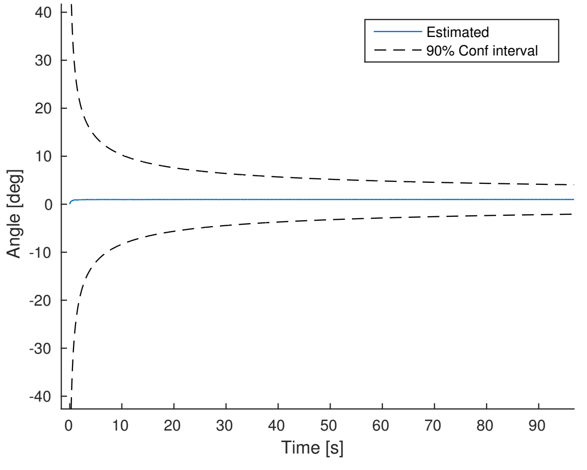

Figure 4.8: *Pitch estimate with a 90% confidence interval for the simulation of the two accelerometer method using measurements with noise.*

Filter parameters

The observation covariance for the simulation of the two accelerometer method was chosen to be

$$R = 10^3 \cdot \begin{pmatrix} 1 & 0 \\ 0 & 1 \end{pmatrix} \tag{4.9}$$

and the process noise covariance as $Q = 10^{-10}$. This choice was made in order to make the filter produce a pitch estimate characterised by low variance. The initial state of the pitch angle was $x_0 = \theta_{g,0} = 0$ and the initial covariance was chosen as $P_0 = 0.5$.

4.4 Map data

The method where map data is used to augment the one accelerometer method has been simulated. The simulated data was, as previously described, generated through the measurement equations described in chapter 3.

4.4.1 Simulation without noise

Figure 4.9 and table 4.9 shows the results of simulating the one accelerometer method augmented with map data without measurement noise. The figure clearly shows that both the road slope and pitch angles quickly converge to the correct values.

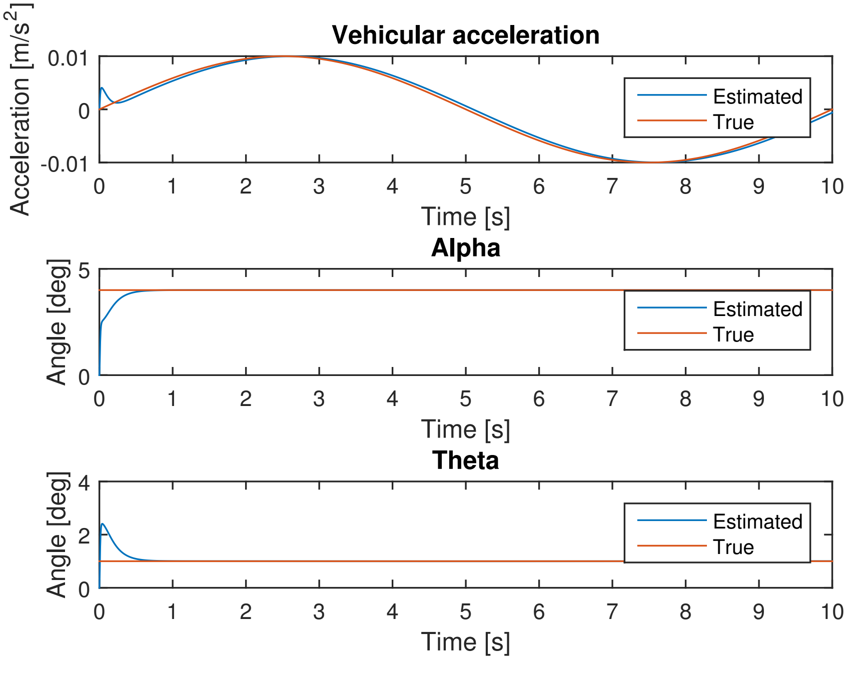

Figure 4.9: *Simulation results when simulating map based pitch estimation without noise.*

	Mean estimate [°]	Ground truth [°]
Pitch	1.00	1
Road slope	4.00	4

Table 4.9: *Mean of pitch estimate and ground truth from simulation of map based pitch estimation metod.*

Filter parameters

The observation and process covariance matrices were chosen as

$$R = 10^6 \cdot \begin{pmatrix} 1 & 0 & 0 & 0 \\ 0 & 1 & 0 & 0 \\ 0 & 0 & 1 & 0 \\ 0 & 0 & 0 & 1 \end{pmatrix} \tag{4.10}$$

and

$$Q = \begin{pmatrix} 1 & 0 & 0 \\ 0 & 1 & 0 \\ 0 & 0 & 1 \end{pmatrix}. \tag{4.11}$$

The initial states and covariance was chosen, as in previous simulations, to be

$$x_0 = \begin{pmatrix} \dot{v}_0 \\ \alpha_0 \\ \theta_0 \end{pmatrix} = \begin{pmatrix} 0 \\ 0 \\ 0 \end{pmatrix} \tag{4.12}$$

and

$$P_0 = 0.5 \cdot \begin{pmatrix} 1 & 0 & 0 \\ 0 & 1 & 0 \\ 0 & 0 & 1 \end{pmatrix}. \tag{4.13}$$

The resulting EKF is a relatively slow filter, that does not put weight on different measurements but rather filters all signals mildly.

4.4.2 Simulation with noise

Figure 4.10 and table 4.10 shows the simulation results with noise added in both the acceleromter and vehicular acceleration signals. The Kalman filter produces a pitch estimate that in average over 100 seconds of simulation time is accurate to within two decimals of the actual pitch angle, measured in degrees.

	Mean estimate [°]	Ground truth [°]
Pitch	1.00	1
Road slope	4.00	4

Table 4.10: *Results from simulation of map based pitch estimation method with noise in accelerometer and vehicular acceleration measurements. Mean estimate calculated from 4 seconds and onward during a 100 second simulation.*

Figure 4.11 shows the pitch estimate with a confidence interval of 90%. As can be seen in the figure, the confidence interval is much closer around the pitch estimate for the map based pitch estimation method than for the one accelerometer method.

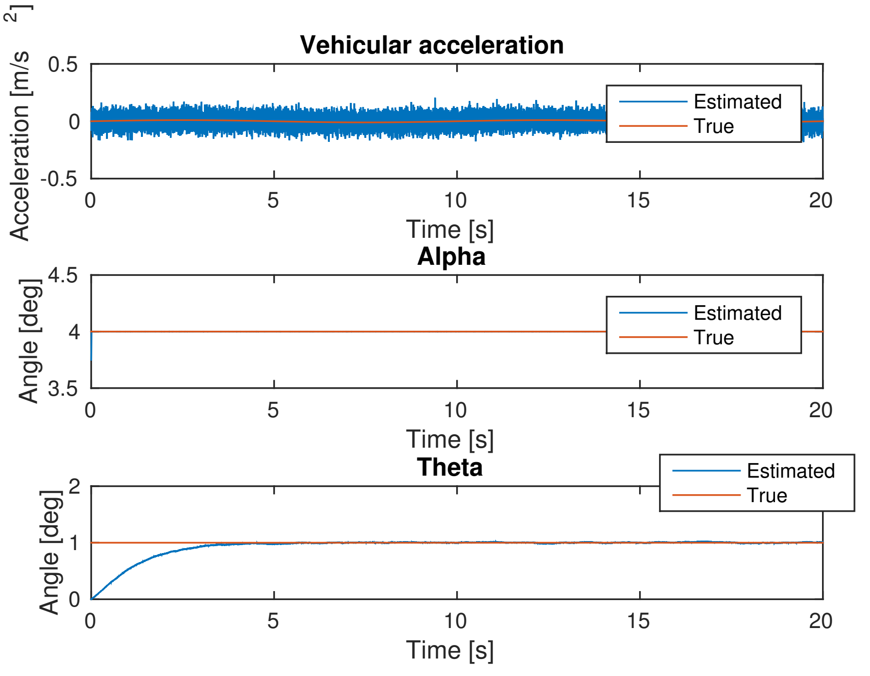

Figure 4.10: *Simulation results for the map based pitch estimation method with noise in both accelerometer axes and vehicular acceleration.*

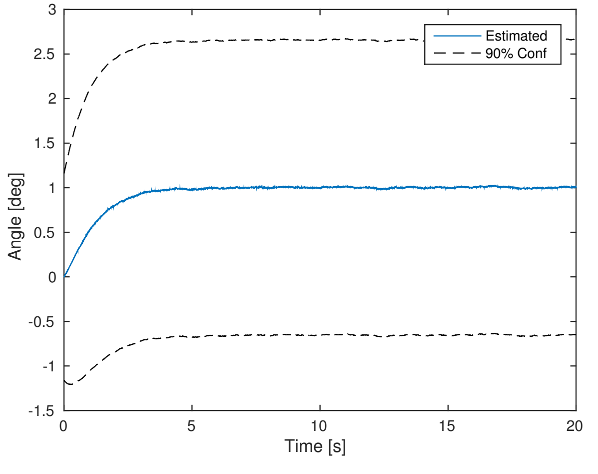

Figure 4.11: *The pitch estimate of the simulation of the map based pitch estimation method together with a 90% confidence interval*

Filter parameters

The observation and process covariance matrices were chosen as

$$R = 10^6 \cdot \begin{pmatrix} 1 & 0 & 0 & 0 \\ 0 & 1 & 0 & 0 \\ 0 & 0 & 10^{-4} & 0 \\ 0 & 0 & 0 & 10^{-7} \end{pmatrix} \tag{4.14}$$

and

$$Q = \begin{pmatrix} 1 & 0 & 0 \\ 0 & 1 & 0 \\ 0 & 0 & 10^{-4} \end{pmatrix}. \tag{4.15}$$

The initial states and covariance was chosen, as in previous simulations, to be

$$x_0 = \begin{pmatrix} \dot{v}_0 \\ \alpha_0 \\ \theta_0 \end{pmatrix} = \begin{pmatrix} 0 \\ 0 \\ 0 \end{pmatrix} \tag{4.16}$$

and

$$P_0 = 0.5 \cdot \begin{pmatrix} 1 & 0 & 0 \\ 0 & 1 & 0 \\ 0 & 0 & 1 \end{pmatrix}. \tag{4.17}$$

These parameters results in a filter that will rely heavily on the measurement signal from the external road slope signal. Further, it assumes the vehicular acceleration signal to contain less noise than the accelerometer signals. Finally, the assumption of a constant vehicle pitch angle θ in the dynamic update of θ is assumed to be reliable, thus suppressing swift shifts in the vehicle pitch estimate.

5

Implementation and results

In order to implement the estimation theory described in chapter 3, the software used was MATLAB. This choice was made due to the power of the MATLAB language in signal processing. The implementation was done in two steps. Firstly, the data was collected from an actual truck while performing tests, secondly, the data was analysed offline. The results of the offline analysis for each of the three methods of pitch estimation are presented in this chapter.

5.1 Evaluation methods

Tests that are performed on the different pitch estimation methods were conducted using a truck that had an air suspension system. This came with two major advantages. Firstly, the air spring suspension system allows for a pitch angle to be determined by the driver. Secondly, a truck with an air spring suspension also has two level sensors measuring the distance between the axle and chassis for the front and rear axles respectively.

These design features allows for tests to be easily performed. Rather than using a truck with leaf spring suspension that would have to be loaded in order to achieve the desired pitch angle, the angle can be set and changed with ease between tests. Further, the level sensors can be used for deriving the actual pitch angle of the vehicle. This can then be used as a reference for comparison with the developed methods.

Figure 5.1 shows an HDV using two level sensors. The figure shows the distances a and b respectively as being measured from the ground to the chassis. In actuality the distances measured are between the wheel axle and the chassis. The geometry for obtaining the pitch angle is however the same. Equation (5.1) shows how to extract the vehicle pitch angle from the level sensor measurements.

$$\theta = \arctan \frac{a - b}{L} \tag{5.1}$$

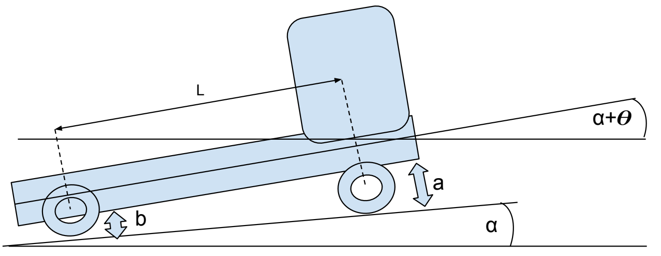

Figure 5.1: *Truck equipped with two level sensors.*

5.2 One accelerometer method

The Kalman filter used for the implementation of the one accelerometer method bears great resemblance to that used for simulation in chapter 4.

5.2.1 Filter tuning and parameters

The filter is tuned in such a way as to rely heavily on the vehicular acceleration while still filtering it in order to avoid the unwanted high frequency noise present. Further, the filter is tuned in such a way that it assumes changes in road slope and vehicle pitch are low frequency events. This method of filter tuning was chosen due to its success in simulation.

The observation and process covariance matrices were chosen as

$$R = 10^4 \cdot \begin{pmatrix} 1 & 0 & 0 \\ 0 & 1 & 0 \\ 0 & 0 & 10^{-4} \end{pmatrix} \tag{5.2}$$

and

$$Q = \begin{pmatrix} 1 & 0 & 0 \\ 0 & 1 & 0 \\ 0 & 0 & 10^{-4} \end{pmatrix}. \tag{5.3}$$

The initial states and covariance was chosen, as previously in simulation, to be

$$x_0 = \begin{pmatrix} \dot{v}_0 \\ \alpha_0 \\ \theta_0 \end{pmatrix} = \begin{pmatrix} 0 \\ 0 \\ 0 \end{pmatrix} \tag{5.4}$$

and

$$P_0 = 0.5 \cdot \begin{pmatrix} 1 & 0 & 0 \\ 0 & 1 & 0 \\ 0 & 0 & 1 \end{pmatrix}. \tag{5.5}$$

5.2.2 Test results

In order to evaluate the one accelerometer method, data was collected while driving on the Scania test track. Figure 5.2 shows the vehicular acceleration as well as the road slope and pitch angle estimates from the one accelerometer method during one such test. As can be seen, the vehicle acceleration is heavily filtered. Further, it is apparent that both the road slope and vehicle pitch angle estimates does not converge to ground truth. This is particularly obvious in the case of the vehicle pitch angle, as there is an actual reference for this variable.

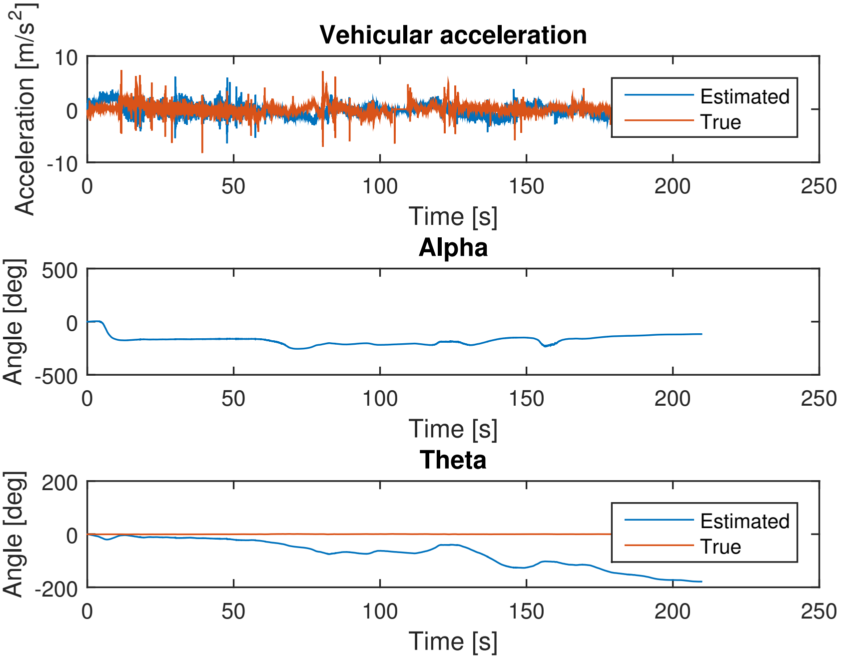

Figure 5.2: *Results from implementation of the one accelerometer method*

Figure 5.3 shows the pitch angle estimate of the one accelerometer method from the implementation on an actual truck together with a 90% confidence interval. The confidence interval is, as it was in simulation, rather wide around the diverging pitch estimate.

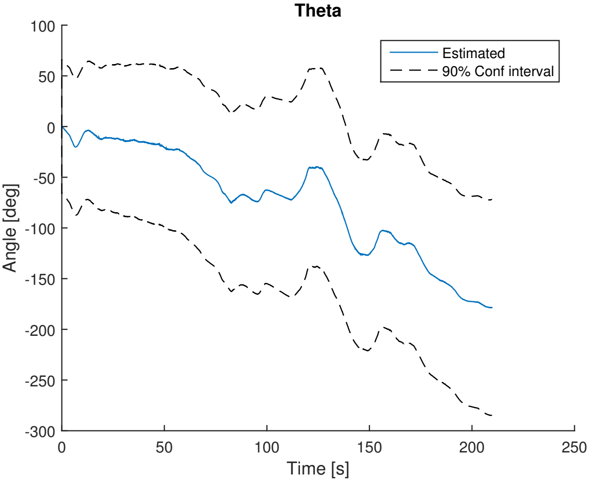

Figure 5.3: *The pitch estimate of the one accelerometer method with a 90% confidence interval*

5.3 Two accelerometer method

The two accelerometer method was evaluated using data collected while the vehicle was at standstill. In order to obtain accelerometer data from the rear axle of the vehicle, an electronic control unit, denoted ECU, was mounted to the rear axle. The ECU is of the same type as one that is mounted on the frame of all Scania vehicles. It contains an accelerometer and provides an interface through which data can easily be recorded.

5.3.1 Filter tuning and parameters

The filters for the frame and axle mounted accelerometer of the two accelerometer method were tuned to be relatively slow. Since the test carried out was done with the vehicle at standstill, the filter is tuned to be faster than in simulation. This was done as to more clearly demonstrate results from the test, which could otherwise be filtered out by a slower filter.

The observation noise covariance was chosen as

$$R = 10 \cdot \begin{pmatrix} 1 & 0 \\ 0 & 1 \end{pmatrix} \tag{5.6}$$

and the process noise covariance as $Q = 10^{-6}$. Further, the initial state was $x_0 = \theta_{g,0} = 0$ and the initial covariance was $P_0 = 0.5$.

5.3.2 Test results

Figure 5.4 shows the results from the pitch estimates for the two accelerometer method with the vehicle at standstill with the engine idling. As can be seen, both the rear axle mounted and the frame mounted accelerometers show a significant change in pitch angle. This was upon closer inspection found to be due to the inherent design of the suspension system of the Scania trucks. As the suspension height is changed, the rear axle will rotate.

Figure 5.5 shows the frame pitch estimate from the two accelerometer method together with a 90% confidence interval.

5.4 Map data

The one accelerometer method augmented with road slope data from a map database has been evaluated through tests performed on public roads rather than on the Scania test track. This was done due to the fact that there is, at the time of writing, no road slope data available for the test track at Scania.

5.4.1 Calibration

An imperfect mounting of the accelerometer to the frame of the vehicle would result in the pitch estimate being biased by an angle corresponding to the angle

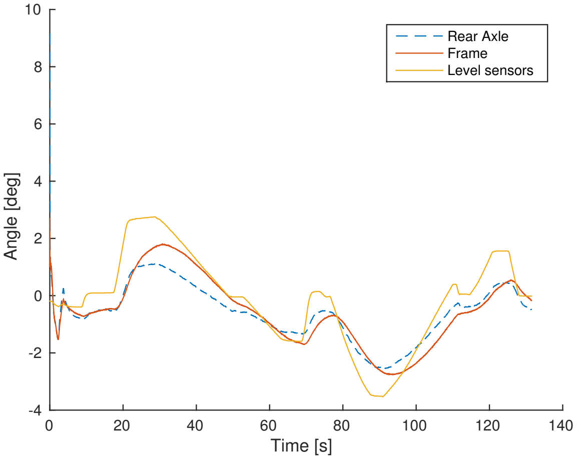

Figure 5.4: *Results from the two accelerometer method with the vehicle at standstill*

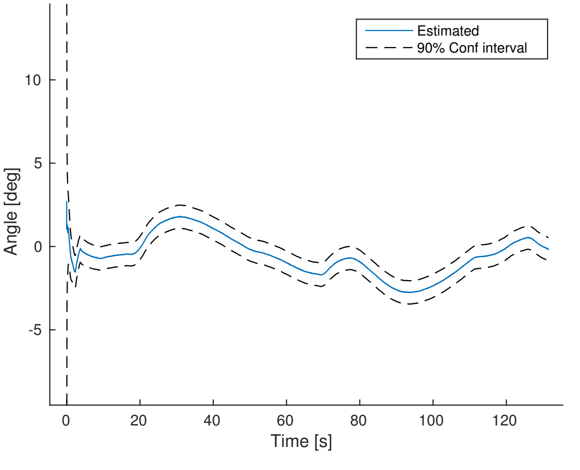

Figure 5.5: *The pitch estimate of the frame mounted accelerometer from the two accelerometer method with a 90% confidence interval*

at which the accelerometer is mounted on the frame. In order to find any such mounting errors, data was for a brief period of time recorded with the vehicle at standstill. The difference between the actual pitch angle and the pitch angle estimate will in this case correspond to the mounting error of the accelerometer. This is due to the fact that there is no dynamic acceleration to affect the estimate. Figure 5.6 shows the mounting error as the vehicle is at stand still on a road with a known road inclination. As can be seen in the figure, the pitch estimate converges toward a mounting error of 0.78°.

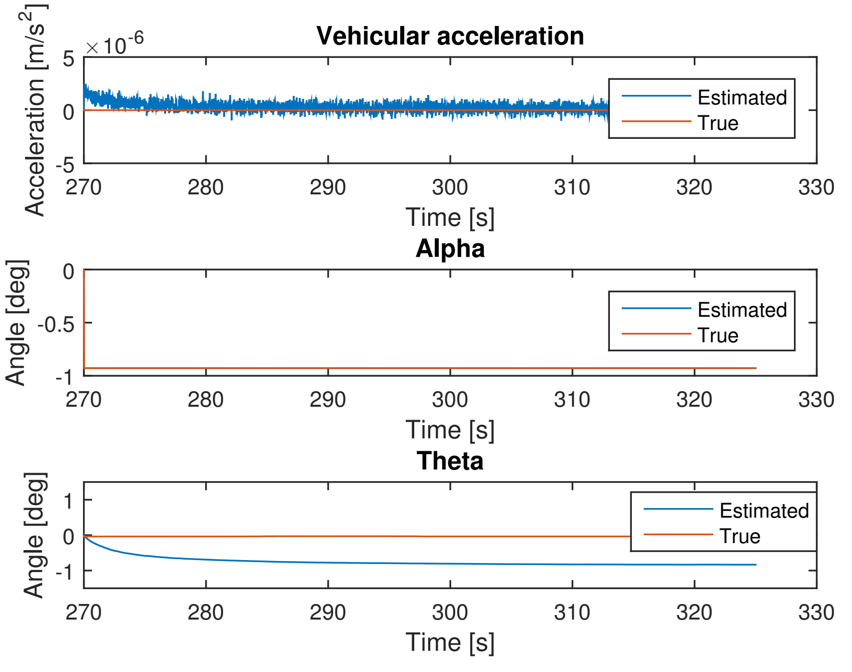

Figure 5.6: *Calibration results for accelerometer mounting errors using the map based pitch estimation method*

5.4.2 Data selection

The first plot in figure 5.7 shows the speed profile of one of the tests. In order to get the best data possible, only parts of the recorded data containing a minimum of accelerations was used in the pitch estimation. This data selection was done in order to minimise the effect of dynamic accelerations on the pitch estimate. The second plot in figure 5.7 shows the speed profile of the data selection used for pitch estimation. As can be seen, the speed is mainly kept constant, as would be expected when driving on larger roads and highways.

5.4.3 Filter tuning and parameters

In order to estimate the vehicle pitch angle, a slow filter which does not rely to heavily on the accelerometer measurements. The observation covariance noise

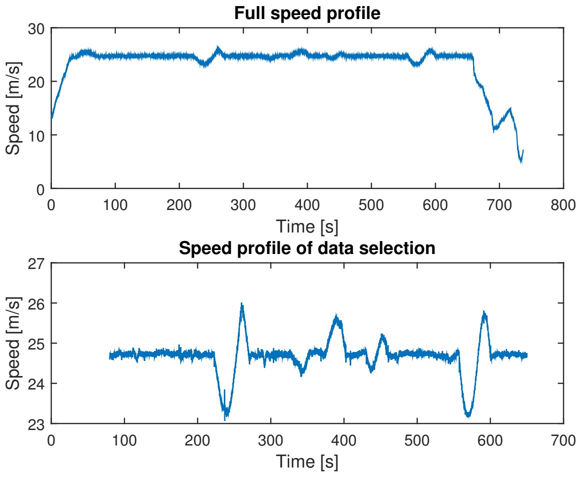

Figure 5.7: *Speed profile of a complete test compared with the speed profile of the data selected for pitch estimation using the map based pitch estimation method*

matrix was tuned to be the diagonal matrix

$$R = 10^5 \cdot \begin{pmatrix} 1 & 0 & 0 & 0 \\ 0 & 1 & 0 & 0 \\ 0 & 0 & 10^{-3} & 0 \\ 0 & 0 & 0 & 10^{-5} \end{pmatrix}. \tag{5.7}$$

This will make the filter rely on the road slope measurements from the map data whereas the accelerometer data is assumed to contain significant amounts of noise. Further, the vehicular acceleration measurements are considered as more reliable than the accelerometer readings. Using a diagonal matrix R also means that an assumption is made that there is no cross-correlation between the different measurements.

The process covariance noise matrix Q was

$$Q = \begin{pmatrix} 1 & 0 & 0 \\ 0 & 1 & 0 \\ 0 & 0 & 10^{-8} \end{pmatrix} \tag{5.8}$$

which assumes a very low amount of process noise on the pitch angle θ. Since θ is assumed to be constant in the time update of the EKF, this will make the filter unresponsive to the fast pitch dynamics involved in events such as road bumps and hard braking. The initial covariance matrix was initialised as

$$P_0 = 0.5 \cdot \begin{pmatrix} 1 & 0 & 0 \\ 0 & 1 & 0 \\ 0 & 0 & 1 \end{pmatrix} \tag{5.9}$$

in order to set a reasonable uncertainty on the initial states allowing the states to drift from the initial states x_0 without diverging. Further, the states were initialised as per

$$x_0 = \begin{pmatrix} \dot{v}_0 \\ \alpha_0 \\ \theta_0 \end{pmatrix} = \begin{pmatrix} 0 \\ 0 \\ 0 \end{pmatrix} \tag{5.10}$$

since both pitch and road slope angles are initially unknown, but close to zero.

5.4.4 Test results

Table 5.1 and figure 5.8 shows the resulting vehicle pitch estimate when using the map based pitch estimation method. As can be seen, the vehicle pitch estimate contains noise, but is unbiased around the actual pitch angle of the vehicle. The main deviations from the actual pitch angle occurs during periods of vehicular acceleration that is nonzero.

	Mean estimate from 500 seconds [°]	Mean ground truth [°]
Pitch	0.772	0.707
Road slope	0.003	0.003
	Mean estimate from 100 seconds [°]	Mean ground truth [°]
Pitch	0.821	0.709
Road slope	-0.054	-0.016

Table 5.1: *Mean values of state estimates from the EKF and mean of ground truth values for the implementation results of the map based pitch estimation method. Mean values are calculated from 100 and from 500 seconds into the measurement and forward.*

Figure 5.9 shows the pitch estimate of the map based pitch estimation method together with a 90% confidence interval. Similarly to the simulated result, it can be seen that the confidence interval of the pitch estimate is more narrow than when implementing the one accelerometer method.

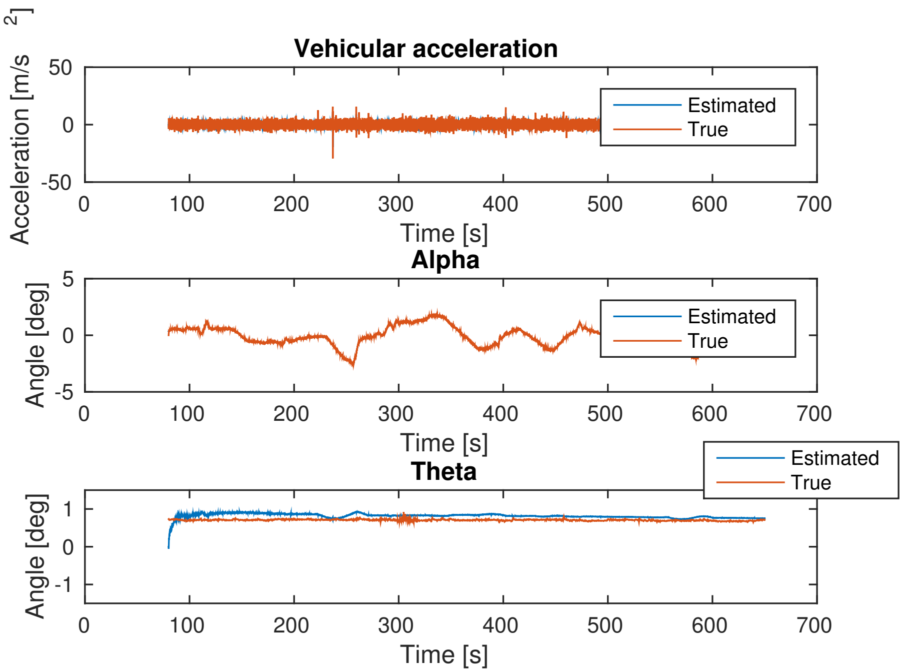

Figure 5.8: *Results from the offline implementation of the map based pitch estimation method*

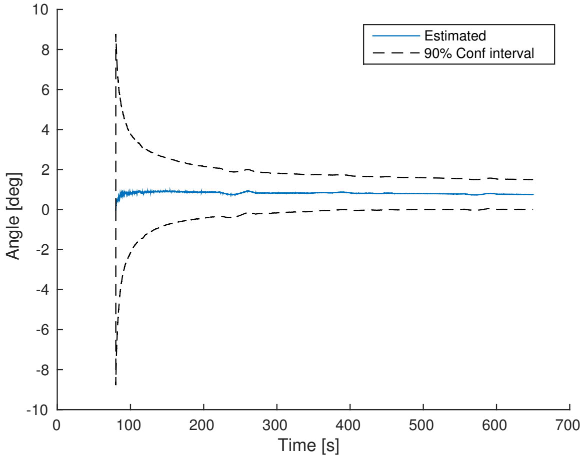

Figure 5.9: *The vehicle pitch estimate from the map based estimation method with a 90% confidence interval*

6 Conclusions

Three main methods for estimating the vehicle pitch of heavy duty trucks have been developed and evaluated. A method using only an accelerometer mounted on the frame of the HDV in combination with the vehicle acceleration has been presented. This method would have been a standalone solution only using existing vehicle sensors for estimating the vehicle pitch. It is however not feasible to implement this method due to the quality and noise sensitivity of automotive grade accelerometers as used in this thesis. This becomes clear when comparing the results from the simulation with the results from the implementation of the one accelerometer method. In simulation, it was shown that the method is viable in an ideal situation without noise. When increasing the noise present in the measurements to realistic levels, the vehicle pitch estimate deteriorated rapidly. Results from the implementation of the one accelerometer again validates the conclusion that the one accelerometer method is too sensitive to measurement noise to be viable as a pitch estimation method.

Further, a method for estimating the vehicle pitch using two accelerometers has also been presented. The accelerometers would be mounted in such a way that one accelerometer would measure the pitch of the vehicle frame relative to gravity. The second accelerometer would then be mounted on the wheel axle, thus providing an estimate of the road slope. This method showed great promise in precision and simplicity but was shown to not be possible to implement in practice as the rear axle of the vehicle rotates when the suspension is compressed. Mounting an accelerometer in such a way as to find the road slope is thus not possible due to the construction of the suspension system on Scania trucks.

Finally, a method for vehicle pitch estimation has been presented based on a combination of vehicular acceleration, accelerometer measurements and a map based database of road slope. This method has the advantage of not needing any non-standard truck sensors while displaying a high degree if accuracy as shown in the test results. It is however not a standalone solution as the map based road slope is not available on all roads. Further, the global positioning system needs to be able to acquire a signal for the method to work.

Thus, the map based vehicle pitch estimation method could be combined with other pitch estimation methods in order to augment the vehicle pitch estimate in the situations where the map based method is capable of providing a pitch estimate. A combination of methods could for instance include a pitch estimation based on only one level sensor on the rear axis as described in chapter 1. This method will give an acceptable pitch estimate in all possible conditions and the map based vehicle pitch estimation could then step in and provide a high accuracy estimate when possible.

The pitch estimation could theoretically be improved upon further with the use of a longitudinal vehicle model as described in section 1.3.7. A model such as this could if used correctly allow the Kalman filters to estimate the vehicular acceleration with better precision than when just using it as a measured value. The problems described pertaining to unknown variables such as vehicle weight however makes this solution impossible to implement with the information at hand in this thesis.

6.1 Future work

Future work include continued testing and validation of the map based pitch estimation method. It is possible that a more aggressively selective approach when selecting the data to be used in the map based pitch estimation algorithm would further increase the pitch estimate accuracy. For the future development of the automatic headlight levelling, the map based vehicle pitch estimation method needs to be implemented on line on a truck.

Further, a thorough investigation into the limitations of the map based pitch estimation method is an essential next step in the development of this method. The limitations would most likely include both the performance of the accelerometer and the reliability and availability of GPS measurements. Accelerometer performance most likely changes with different conditions such as temperature and age of the accelerometer.

Other sensors, such as radar distance sensors are also becoming increasingly cheap and accurate. Future work could therefore include an investigation into the new possibilities these and other sensors might offer for the purpose of vehicle pitch estimation.

Bibliography

[1] Hong S Bae, Jihan Ryu, and J Christian Gerdes. Road grade and vehicle parameter estimation for longitudinal control using gps. In *Proceedings of the IEEE Conference on Intelligent Transportation Systems*, pages 25–29, 2001. Cited on page 3.

[2] Hamdi Bawaqneh. Virtual vehicle pitch sensor. Master's thesis, Linköping University, 2011. Cited on page 3.

[3] Axel Elmelid. Automatisk nivåreglering av strålkastare. Master's thesis, Uppsala Universitet, 2012. Cited on pages 2 and 3.

[4] Ritzén Emil. Adaptive vehicle weight estimation. 2011. URL `https://login.e.bibl.liu.se/login?url=https://search.ebscohost.com/login.aspx?direct=true&db=edsbas&AN=edsbas.ftciteseerx.oai.CiteSeerX.psu.10.1.1.29.9440&site=eds-live&scope=site`. Cited on page 9.

[5] Michael T Gansler. Apparatus and method for pitch state estimation for a vehicle, July 12 2011. US Patent 7,979,179. Cited on page 3.

[6] Fredrik Gustafsson. *Statistical sensor fusion*. Studentlitteratur, Lund, 2012. ISBN 9789144077321. Cited on pages 2 and 12.

[7] Lennart Ljung. *Modellbygge och simulering*. Studentlitteratur, Lund, 2004. ISBN 9789144024431. Cited on page 2.

[8] F. Landis Markley. Humble problems. 2006. URL `https://login.e.bibl.liu.se/login?url=https://search.ebscohost.com/login.aspx?direct=true&db=edsbas&AN=edsbas.ftnasantrs.oai.casi.ntrs.nasa.gov.20060012294&site=eds-live&scope=site`. Cited on page 18.

[9] F.Landis Markley. Attitude determination using vector observations and the singular value decomposition. *Journal of the Astronautical Sciences*, 36(3):245–258, 1988. ISSN 00219142. URL `https://login.e.bibl.liu.se/login?url=https://search-ebscohost-com.e.bibl.`

liu.se/login.aspx?direct=true&db=edselc&AN=edselc.2-52.0-0024037688&site=eds-live&scope=site. Cited on page 18.

[10] T Massel, EL Ding, and M Arndt. Identification of road gradient and vehicle pitch angle. In *Proceedings of the 2004 IEEE International Conference on Control Applications*, pages 1284–1289, 2004. Cited on page 3.

[11] Per Sahlholm. Distributed road grade estimation for heavy duty vehicles. 2011. Cited on pages 2, 3, 4, and 8.

[12] P. Shakouri, A. Ordys, M. Askari, and D.S. Laila. Longitudinal vehicle dynamics using simulink/matlab. In *Control 2010, UKACC International Conference on*, pages 1–6, Sept 2010. doi: 10.1049/ic.2010.0410. Cited on page 2.

[13] S Söhner, T Schaal, P Heimpel, J Bortolazzi, and W Stork. Automatic headlamp setting (ahs). In *Proceedings of the 2013 International Symposium on Automotive Lighting*, pages 70–79, 2013. Cited on page 4.

[14] Atsushi Toda and Hideaki Takeuchi. Automatic automobile headlamp leveling device, February 19 2002. US Patent 6,349,251. Cited on page 3.

[15] Robert R Turnbull, Robert C Knapp, and Eric J Walstra. Headlight control system utilising information from a microwave receiver, October 15 2002. US Patent 6,465,963. Cited on page 3.

[16] United Nations Unece. Installation of lighting and light-signalling devices on motor vehicles, 2016. URL http://www.unece.org/trans/main/wp29/wp29regs41-60.html. Regulation 48, rev 12. Cited on page 1.